



## Review

The study of Li effect on the microstructure and tensile properties of cast Al–Mg<sub>2</sub>Si metal matrix compositeR. Khorshidi<sup>a</sup>, A. Honarbakhsh Raouf<sup>a</sup>, M. Emany<sup>b,\*</sup>, J. Campbell<sup>c</sup><sup>a</sup> Department of Materials, Faculty of Engineering, Semnan University, Semnan, Iran<sup>b</sup> School of Metallurgy and Materials, University of Tehran, 11365-4563, Tehran, Iran<sup>c</sup> Department of Metallurgy and Materials, University of Birmingham, Edgbaston B15 2TT, UK

## ARTICLE INFO

## Article history:

Received 1 December 2010

Received in revised form 3 July 2011

Accepted 5 July 2011

Available online 14 July 2011

## Keywords:

Al–Mg<sub>2</sub>Si composite

Microstructure

Mechanical properties

Bifilms

## ABSTRACT

This study is undertaken to investigate the effect of different concentrations of Li (0.03–0.35%) on the microstructure and tensile properties of Al–15 wt.%Mg<sub>2</sub>Si in situ metal matrix composite. The results showed that 0.15 wt.% Li addition changes the morphology of primary Mg<sub>2</sub>Si from irregular or dendritic to polyhedral shape and its average particle size decreases from 32 μm to 4 μm. Microstructural observations also depicted that the morphology of the eutectic Mg<sub>2</sub>Si phase alters from flake-like to coral-like. Further investigations on tensile tests revealed optimum Li level (0.15%) for improving both UTS and elongation values. A study of the fracture surfaces via scanning electron microscope (SEM) revealed a brittle mode of failure in unmodified composite however the addition of 0.15%Li converts the fracture behaviour to ductile. The behaviour is explained in terms of the presence of oxide bifilms in the liquid Al alloy.

© 2011 Elsevier B.V. All rights reserved.

## Contents

1. Introduction .....	9026
2. Experimental procedure .....	9027
3. Results .....	9027
3.1. Microstructural studies .....	9027
3.1.1. Effects of Li addition on primary Mg <sub>2</sub> Si particles .....	9027
3.1.2. Effect of Li addition on pseudo-eutectic matrix .....	9027
3.2. Tensile properties .....	9028
3.3. Fractography .....	9028
4. Discussion .....	9029
5. Conclusions .....	9033
Acknowledgment .....	9033
References .....	9033

## 1. Introduction

Aluminum metal matrix composites as a class of advanced engineering materials have been developed for high-performance applications because of their low density, excellent castability, good wear resistance and remarkable physical properties [1–7]. Particulate metal matrix composites (PMMCs) are one type of MMC which has attracted attention due to their inherent isotropic properties,

ease of manufacture and lower costs [8,9]. Among the numerous methods for PMMCs, in situ processes produce good particle wetting, even distribution of the reinforcing phase and thermodynamically stable systems [2,7]. This technique has significant potential for simplicity of production because it simply forms itself during freezing. Recently, in situ Al–Mg<sub>2</sub>Si composites have been proposed as a potentially useful new group of PMMCs which contain a large amount of hard particles of Mg<sub>2</sub>Si in a ductile Al-matrix [10,11]. The intermetallic compound Mg<sub>2</sub>Si is a stable phase in the binary Mg–Si system [12] having a high melting temperature, low thermal expansion coefficient (TEC), high elastic modulus, high hardness and low density. The Al–Mg<sub>2</sub>Si composite is a typical

\* Corresponding author. Tel.: +98 21 82084083; fax: +98 21 82084083.  
E-mail address: [emamy@ut.ac.ir](mailto:emamy@ut.ac.ir) (M. Emany).

**Table 1**  
Chemical composition of in situ Al–15%Mg<sub>2</sub>Si primary ingots (wt.%).

Si	Mg	Fe	Ni	Zn	Al
5.750	9.650	0.130	0.030	0.009	Bas

example of an ultra light material appropriate for weight-critical applications specially in the aerospace and automotive industries [11,13,14]. Zhang et al. showed that in terms of properties and solidification behaviour, great similarities exist between Mg<sub>2</sub>Si and Si, and between Al–Mg<sub>2</sub>Si and Al–Si systems [7,8].

Unfortunately, in its original as-cast condition, the presence of coarse primary Mg<sub>2</sub>Si particles in the composite matrix leads to poor tensile properties [15]. Clearly therefore, it seems desirable to refine the structure of the MMC to improve the properties [16–18]. The enhancement of mechanical properties may be attained by modifying both primary and secondary Mg<sub>2</sub>Si particles [4,16]. Researches on the microstructural characteristics have been shown that modification of the microstructure can be achieved by a number of modifying agents including K<sub>2</sub>TiF<sub>6</sub> [5], mischmetal [7], strontium [10], Al–P master alloys [16], extra Si [19] or Li [9].

It also increases specific heat and improves cryogenic properties [20]. In previous work, Hadian et al. [9] found that the addition of Li reduces the size of primary Mg<sub>2</sub>Si particles and improves the tensile strength and elongation.

The present work has been carried out to evaluate the effect of different Li concentrations on the microstructure and tensile properties of an in situ hypereutectic Al–15%Mg<sub>2</sub>Si composite.

## 2. Experimental procedure

Al–15%Mg<sub>2</sub>Si composite as primary ingots were prepared in an electrical resistance furnace using a 10 kg clay–graphite crucible using 99.8%Al, 99.9%Mg and 99%Si. After reaching 800 °C, Mg and Si were added into the Al melt (To take account of losses an extra 17%Mg and 7% Si were added above the stoichiometric requirements). Table 1 shows the chemical composition of the melt after stirring and homogenising for 10 min. The chill-cast ‘cylindrical’ sample was analysed by spark emission spectrograph.

The melt was poured into ingot molds to form parent ingots. These were cut to fit a 2 kg capacity SiC crucible and were melted in an electrical resistance furnace. When the temperature reached 750 °C, pure Li wrapped in aluminum foil was added in small increments, to prepare alloys containing 0, 0.03, 0.05, 0.07, 0.1, 0.15, 0.25 and 0.35 wt.%Li. An addition of MgF<sub>2</sub> containing flux powder ensured that the melt surface remained covered. Previous experience indicated that it was necessary to add 20% additional Li to be certain that the target composition was reached. Degassing was conducted by using dry tablets containing C<sub>2</sub>Cl<sub>6</sub> (0.3 wt.% of the molten alloy) for about 3 min. After stirring and cleaning off the dross, the alloys were poured into a steel mould preheated to 200 °C. The mould was made according to the ASTM B 108–03a standard (Fig. 1a). The tensile test specimens were made according to ASTM B557M–02a standard shown in Fig. 1b.

Tensile tests were carried out in a computer controlled MTS tensile testing machine at a constant cross-head speed of 1 mm/min. Specimens for microstructural characterization were sectioned from the gauge length portion of the tensile test castings. Metallographic specimens were polished using standard routines and etched with 0.5% HF for about 15 s at room temperature. Specimens were deeply etched in mixture of 15% NaOH/water solution to remove the Al matrix. Microstructural parameters were determined using an optical microscope equipped with an image analysis system (Clemex Vision, Pro.Ver. 3.5.025). The microstructural characteristics of the specimens were also examined by scanning electron microscopy (SEM) in both Vega SEM with the energy dispersive X-ray analysis (EDX) accessory and Philips XL30 SEM.

In order to the study of Li effect on Al–Mg<sub>2</sub>Si pseudobinary diagram, thermal analysis also carried out for both of the unmodified and 0.15%Li modified samples. On this purpose, two thermocouples (entitled t1 and t2) were placed in the empty molds (similar to Fig. 1). The molds had a wall thickness of 44 mm. The thermocouples were placed at approximately in the center of the casting, i.e., at distances of 85 mm from the casting end. The melt was poured directly from the crucible to minimize temperature loss during pouring. The pouring temperature was approximately 750 °C and the weight of metal sample poured was 200 g. Temperature data was acquired with thermocouples type K at approximately 60 Hz. The diameter of the thermocouple wires was 0.3 mm and the thermocouple tip was in direct contact with the melt. The cooling curves are shown in Fig. 2a–d.

As shown in Fig. 2, the cooling rates for unmodified and 0.15%Li modified MMC castings were approximately 50 and 80 °C/s, respectively.

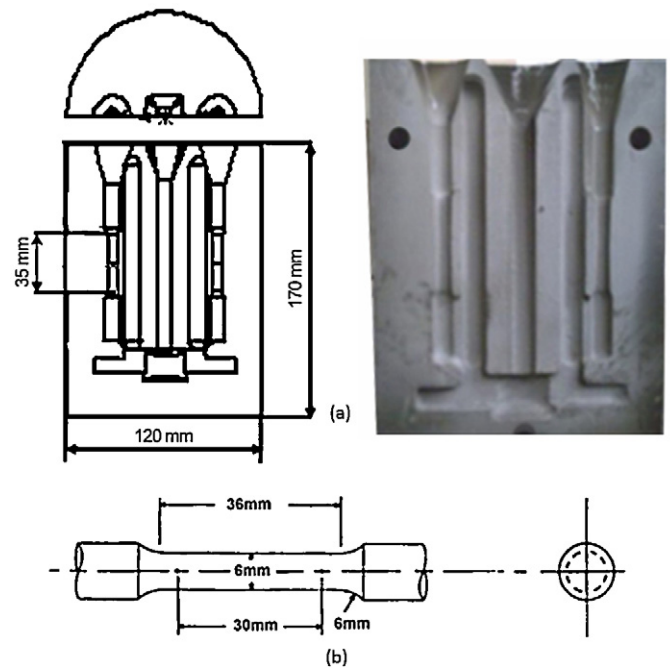


**Fig. 1.** The schematic of: (a) Casting mould and (b) tensile test specimen.

## 3. Results

### 3.1. Microstructural studies

As can be seen in Fig. 3, all the primary particles are surrounded by a layer of  $\alpha$ -Al.

Zhang et al. also proposed that Mg<sub>2</sub>Si particles act as heterogeneous sites for the nucleation of  $\alpha$ -Al [7]. This microstructural characteristic is similar to some of the findings in Al–Si [21] and Mg–Si [22] hypereutectic systems.

#### 3.1.1. Effects of Li addition on primary Mg<sub>2</sub>Si particles

The representative optical microscopy microstructures of the composite with varying Li addition are compared in Fig. 4a–d.

According to the pseudobinary phase diagram of Al–Mg<sub>2</sub>Si system (Fig. 5), the composition of Al–15%Mg<sub>2</sub>Si consists of the primary Mg<sub>2</sub>Si and  $\alpha$ -Al phases.

The dark particles are the primary Mg<sub>2</sub>Si and the bright phase is  $\alpha$ -Al. From Fig. 4a, it is clearly seen that the morphology of the primary unmodified Mg<sub>2</sub>Si particles is irregular, often dendritic, with average size 32  $\mu$ m. Dendritic morphology of particles is expected, since cooling rate in this work is high. Similar dendritic morphology of Mg<sub>2</sub>Si in non-modified Al–Mg<sub>2</sub>Si composite has been reported in the literature [4,11,12]. After 0.15% Li addition, primary Mg<sub>2</sub>Si is seen to be fully polyhedral and its size decreases to 4  $\mu$ m (Fig. 4c). The use of more Li (>0.15 wt.%) does not significantly change the size or morphology of the primary Mg<sub>2</sub>Si as shown in Fig. 4d. The measured particle size and volume fraction of the primary Mg<sub>2</sub>Si phase with varying Li addition are presented in Fig. 6.

It is clear that the Li addition refines the size of the primary Mg<sub>2</sub>Si particles more than 85%, although its volume fraction remains constant with a satisfactorily uniform distribution of primary Mg<sub>2</sub>Si particles in the matrix.

#### 3.1.2. Effect of Li addition on pseudo-eutectic matrix

After the precipitation of the primary Mg<sub>2</sub>Si particles from the liquid alloy, it is obvious from Fig. 5 that the subsequent solidification happens by introducing a layer of  $\alpha$ -Al around the particles and then  $\alpha$ -Al and Mg<sub>2</sub>Si co-solidify in a narrow ternary phase region

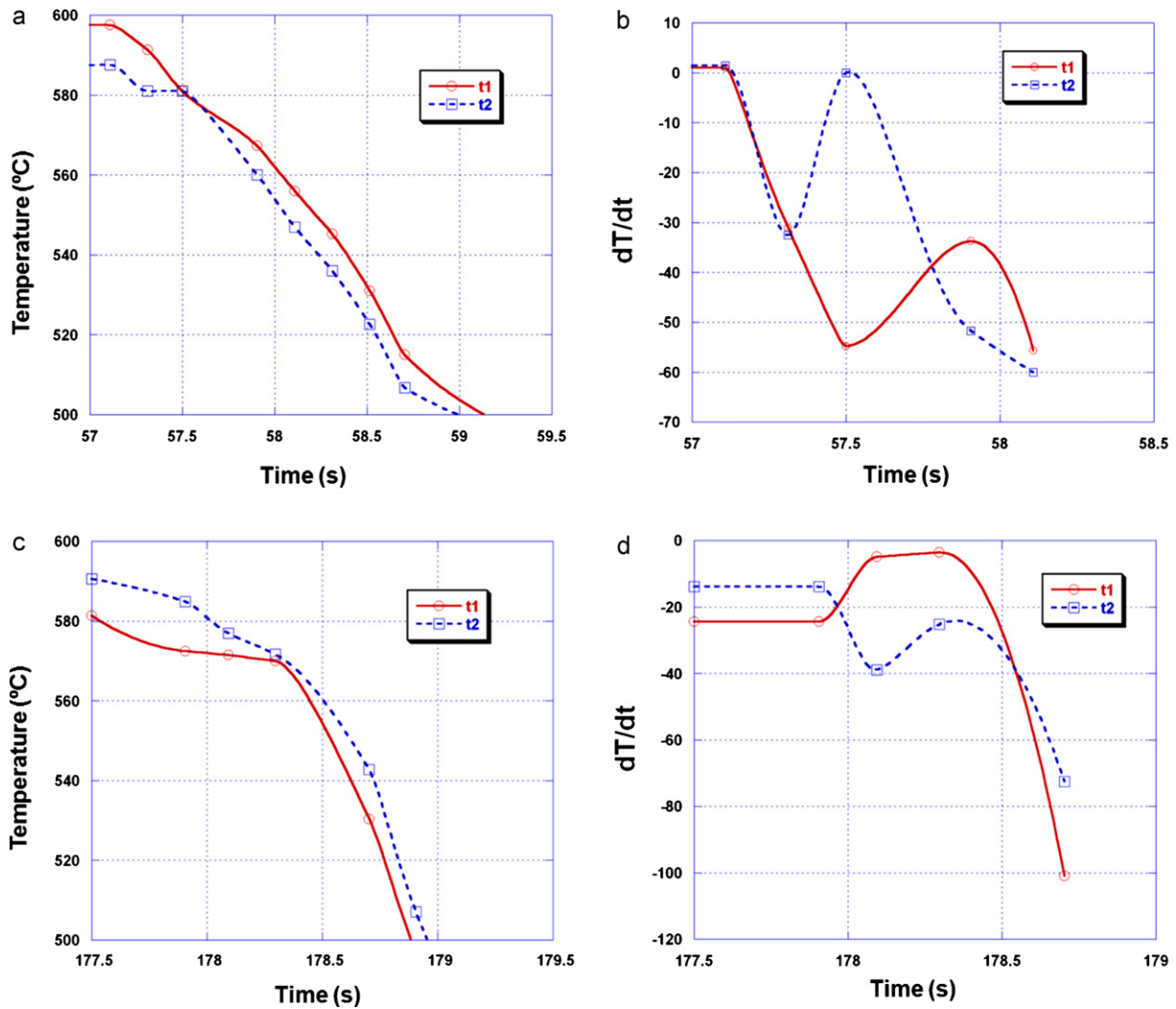


Fig. 2. Cooling curves for (a and b) unmodified and (c and d) 0.15%Li modified composites in the mould similar to Fig. 1.

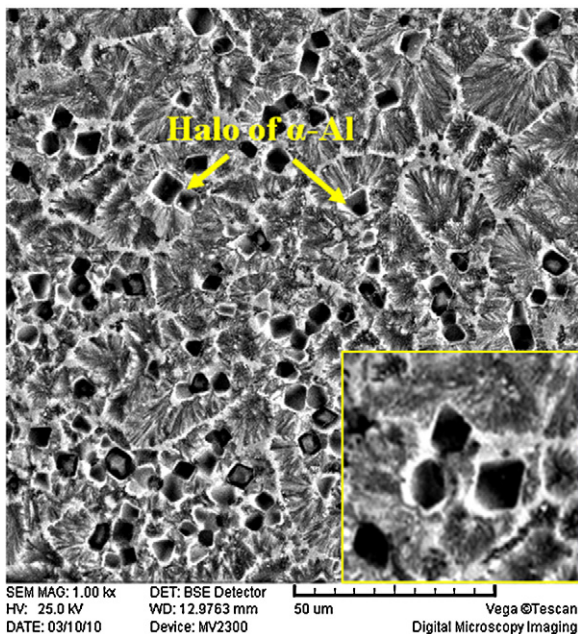


Fig. 3. SEM micrograph shows halo of  $\alpha$ -Al around primary  $Mg_2Si$  particles in 0.15%Li modified Al-15%  $Mg_2Si$  composite.

(Fig. 5). With the addition of 0.15%Li, the number of the primary  $Mg_2Si$  particles is increased and basically, the volume fraction of  $\alpha$ -Al in the matrix increases.

### 3.2. Tensile properties

Fig. 7 depicts the effect of Li modification on the UTS and elongation values of the MMC specimens as a function of added Li contents.

It is evident from Fig. 7 that Li modification has a significant influence on tensile properties of the composite, raising both the UTS and elongation values. In addition, the stress–strain curves of the Li-modified alloys show a serrated yielding behaviour (Fig. 8).

### 3.3. Fractography

Fig. 9a and b exhibit typical fracture surfaces of Al-15 wt.% $Mg_2Si$  composite with and without Li.

From Fig. 9a, both decohered and cracked particles are present simultaneously in the unmodified matrix structure. The eutectic  $Mg_2Si$  in unmodified matrix is clearly shown with arrow (1). Arrow (2) also depicts some decohered particles in matrix structure. The 0.15%Li modified composite contains more cracked particles (arrow 3) with a large amount of fine dimples (arrow 4) which is obviously observed in wide area of face. According to the previous

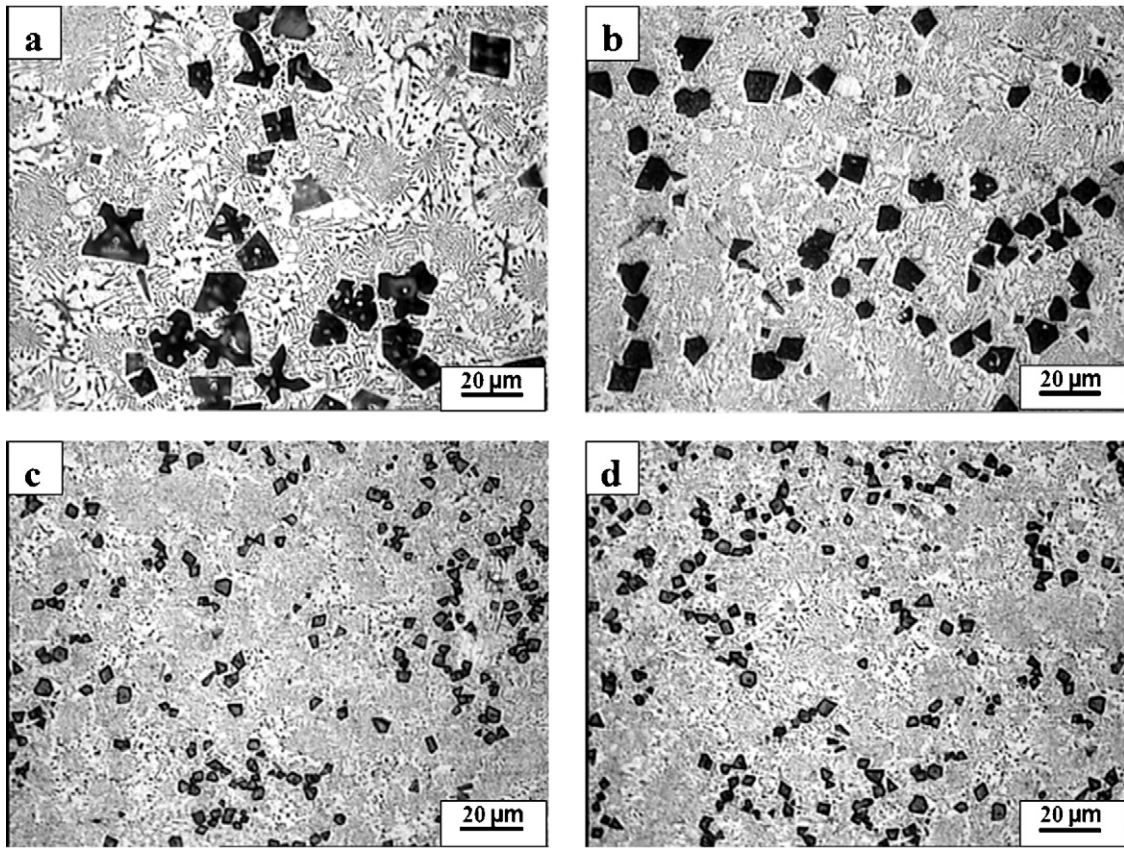


Fig. 4. Optical microscope microstructures of in situ Al-15 wt.%Mg<sub>2</sub>Si composites with Li contents: (a) 0 wt.%, (b) 0.05 wt.%, (c) 0.15 wt.% and (d) 0.25 wt.%.

studies [23], with a decrease in particle size and an increase in fine dimples elongation value rises. Since the most area of fine dimples appear in face of 0.15%Li modified composite, the highest elongation value of 7% attains in this case. Fig. 10a–d shows the fractured faces of the specimens with different concentrations of Li at higher magnification. From Fig. 10a–d, it is clear that both cracked particles and fine dimples are encouraged by increasing Li content.

#### 4. Discussion

The major focus of this study is to develop an understanding of the remarkable behaviour of the Li as an addition to the molten MMC.

The traditional metallurgical explanations for the action of Li are numerous but inconclusive. It is possible that Li might restrict the growth of Mg<sub>2</sub>Si crystal by poisoning growth sites on the surface of the Mg<sub>2</sub>Si nuclei. Since Li is one of the few elements with consider-

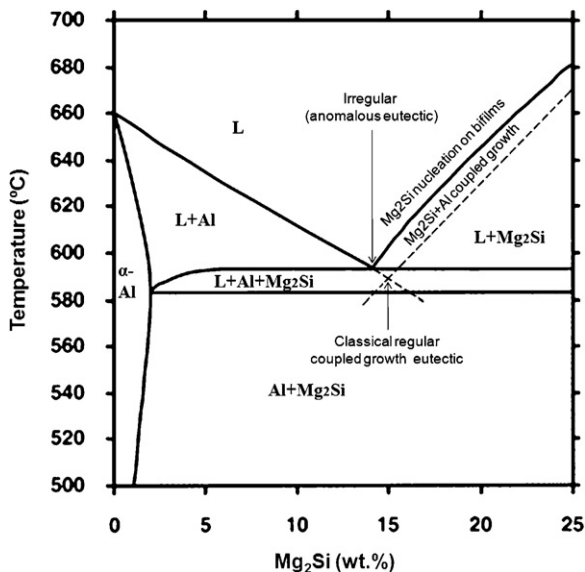


Fig. 5. Equilibrium phase diagram of Al-Mg<sub>2</sub>Si pseudobinary section.

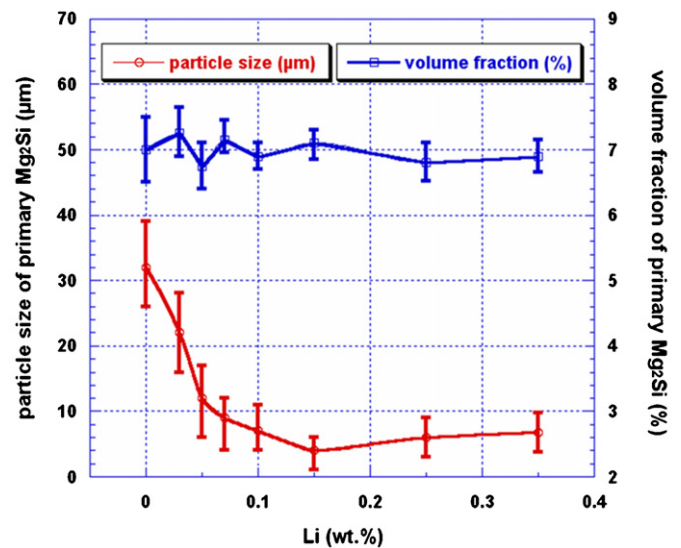


Fig. 6. The size and volume fraction of primary Mg<sub>2</sub>Si particles as a function of Li additions.

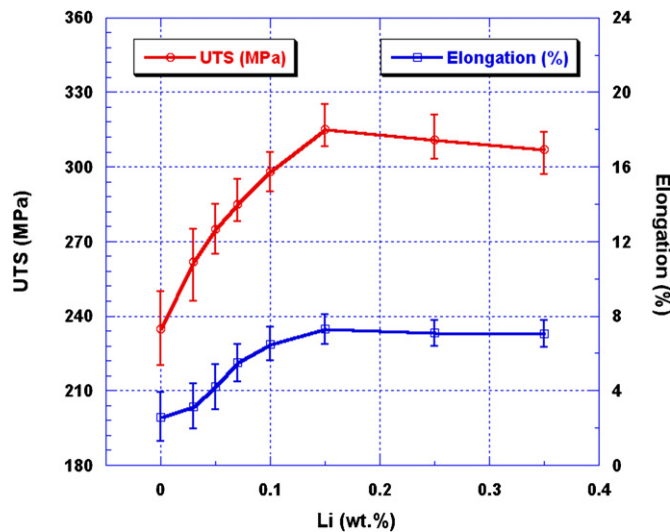


Fig. 7. Tensile properties as a function of added Li.

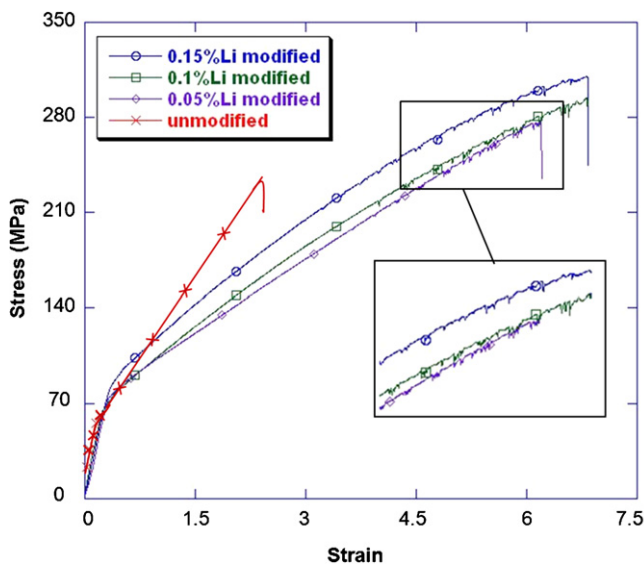


Fig. 8. Serration behaviour in Li-modified tensile results.

able solubility in solid aluminum (4.2 wt.% in binary Al–Li alloy) [20] and has small reactivity with  $Mg_2Si$  phase [20], Li addition may create some distortion in the  $Mg_2Si$  lattice and thus change the surface energy of the  $Mg_2Si$  crystals. There is also a hypothesis that Li may affect on the pseudobinary phase diagram of the Al– $Mg_2Si$  composite and shift the binary eutectic-point into the  $Mg_2Si$  rich side [9]. In addition, Li may decrease the eutectic temperature which basically leads to nucleation enhancement of  $Mg_2Si$  particles during initial stage of solidification. In terms of the failure mechanisms, damage in composites containing particles has been explained as involving two classes of behaviour: particle fracture and particle decohesion [24]. Previous studies [24,25] have emphasised the two major factors appearing to control properties and fracture behaviour are the particle size and the strength of matrix/particle interface, but explanations for these mechanisms by which these factors act has been elusive.

A recent hypothesis that appears to explain the refinement of Al–Si eutectic by Sr addition [26] seems likely to apply also in this alloy system. It seems that Al alloys are generally full of double oxides [27–29] that act both as substrates for the precipitation of second phases (such as  $Mg_2Si$  in this case), and as cracks in the liq-

uid which survive as cracks in the solid. These doubled-over oxide films, known as bifilms, tend to be so thin that they are generally invisible to casual observation. Usually large populations of bifilms are introduced into metals at an early stage of their production. In general their presence has been unsuspected because although they can have large area, they can often be only nanometres thick and not easily detected by conventional non-destructive techniques. The populations of cracks in suspension in liquid metal explains many otherwise inexplicable features of cast products such as porosity, hot tearing, the morphologies of second phases, and impaired reliability of mechanical properties. The fundamental difference between such entrained defects (associated with a macroscopic unbonded interface) and defects and inclusions grown in the melt is seen to be of central significance for the failures of metals by mechanical or corrosion type mechanisms [30]. They are formed simply by the pouring of the liquid metal, since the oxide on the surface becomes entrained, dry top side of the oxide becomes folded against dry top side, resulting in no bonding between these folds, resulting in the double film floating as a crack inside the liquid. In contrast, the outer surfaces of the double films are the original surfaces from which the oxide grew atom by atom on the surface of the liquid, and so will be in perfect atomic contact with the matrix liquid (i.e. is well ‘wetted’).

Large populations of oxide bifilms are to be expected therefore in most Al alloys, residing in suspension in the liquid, in dense clouds as fogs or snowstorms. Internal turbulence in the liquid ensures that the bifilms are ravelled into convoluted, compact forms, so their internal crack is relatively harmless, and properties are relatively high. (Naturally, the properties would be even higher in the absence of bifilms, but this condition is expected to be achieved only rarely, following great care to liquid handling and treatment).

The precipitation of the intermetallic  $Mg_2Si$  on the wetted exterior faces of the bifilms, that appear to act as favoured substrates, explains the phenomena of decohering particles and cracked particles. Cracks through the centres of particles result from particles having formed on both sides of a bifilm. Decohesion of particles from the matrix is explained by the intermetallic having formed on only one side of the bifilm.

Cracks associated with particles are not otherwise easily explained, since the cracks cannot have arisen from the phase change of solidification, since interatomic bonding is enormously strong. Furthermore, the  $Mg_2Si$  particles that have nucleated and grown in situ in the matrix and will therefore be in perfect atomic contact with the matrix. Thus the particle/matrix interface is also expected to be strong and resistant to decohesion. Similarly, intermetallic particles are expected to be strong and rather resistant to cracking except at stresses in the GP region – too high to be developed in a relatively weak Al matrix.

Thus it seems that the  $Mg_2Si$  is likely to precipitate and grow on the wetted exterior interfaces of oxide bifilms. These favourable substrates ensure that the intermetallic nucleates early during cooling, and grows to develop a relatively coarse morphology. It seems probable that the eutectic will also grow on the oxide film substrates. As it grows, the large plate-like morphology of the  $Mg_2Si$  eutectic phase (Fig. 11a), dictated by its diamond cubic lattice, will straighten bifilms, effectively straightening the central crack of the bifilm from its original harmless convoluted form to become more like a normal engineering crack developed by stress. Thus as the population of cracks straighten so mechanical properties will be expected to fall.

Primary  $Mg_2Si$  particles nucleate and grow on the outer, wetted surfaces of the bifilm. Initially, when the  $Mg_2Si$  crystals are no more than a few nanometers thick, the crystals can follow the curvature and creases of the crumpled double film. However, as the crystals grow in thickness, because the rigidity of a beam in bending mode is proportional to its thickness, they quickly develop rigidity. Thus

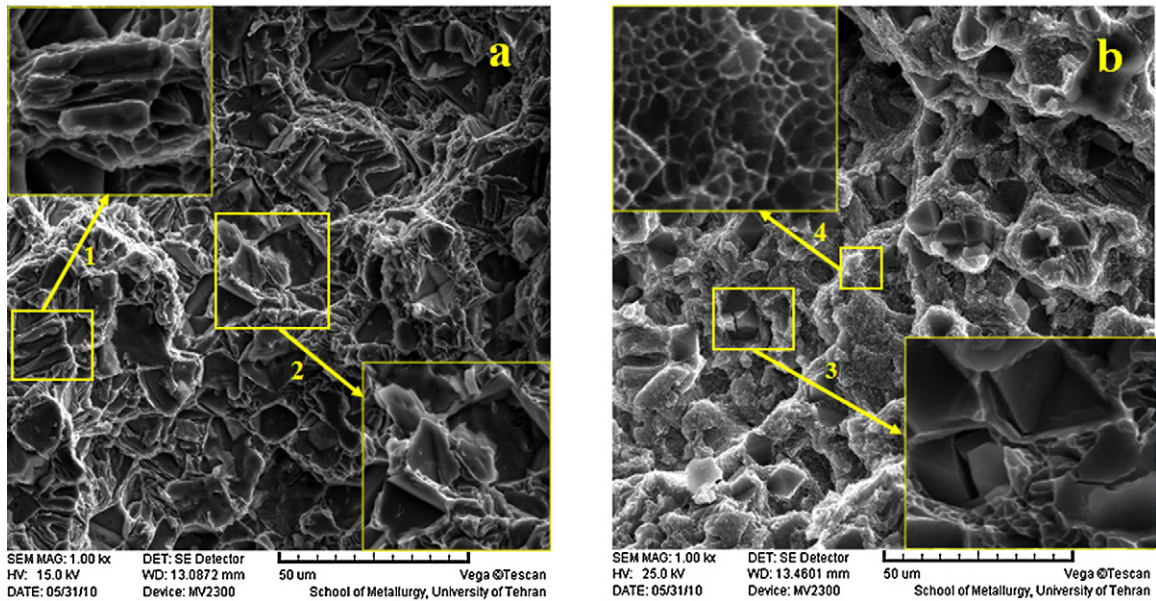


Fig. 9. Tensile fracture surfaces of the Al–15 wt.%Mg<sub>2</sub>Si hypereutectic composite: (a) unmodified and (b) modified by adding 0.15%Li.

as they thicken and rigidize, they force the straightening of the bifilm.

This straightening (or perhaps rather, flattening) of the bifilm cracks explains much of the fractography observed in this study.

Fig. 10a depicts some decohered particles with large facets, suggesting a brittle mode of failure, but in fact confirming the growth of the intermetallic particles and the eutectic phases on the bifilms, flattening them, and thus creating large planar cracks which are naturally opened during the fracture process, thus appearing brittle.

After 0.25%Li addition, much smaller cracked particles appear in the fracture surface (Fig. 10d) possibly indicating some residual formation of particles on bifilms. Even though the bifilms are no longer expected to be extensively straightened, they may still affect tensile failure in their compact convoluted forms, opening and diverting the growth of crack in a rather random irregular manner during fracture, but clearly representing less serious mechanical crack-like defects to reduce properties.

As a direct result of the non-straightening of bifilms after Li addition, the mechanical properties are improved. Both strength and ductility are raised, representing a major explanation of the effect of Li on properties.

The addition of Li (following the analogy of the addition of Sr in Al–Si alloys) seems to render the oxide substrates unfavourable as substrates for precipitation of Mg<sub>2</sub>Si. Thus the melt now continues to cool to new lower temperatures, at which the oxide bifilms finally reach a temperature at which they will act as substrates, or some other nucleation site becomes active. This necessarily is accompanied by refinement of the Mg<sub>2</sub>Si. Furthermore, assuming that the eutectic is also no longer nucleated, and no longer uses the oxide films as substrates for growth, now adopts a growth form as a classical coupled eutectic. Again, in analogy with Al–Si, the eutectic now grows with a fine, fibrous morphology. The coral-like growth results from the intermetallic having to continuously change its growth direction as a result of the influence of its close neighbours. Such changes in direction will be resisted by its strong preferred growth direction as a result of the anisotropy of its lattice, causing it to develop growth faults, which, in the case of Si in the Al–Si alloys, is a high density of twinning defects.

Whereas the coral growth of the eutectic might be assumed to explain the improved mechanical properties, by analogy with the

Sr-refined Al–Si eutectic system, it is also suspected in this case that the refined structure has minimal effect on properties. The raising of yield strength might be explainable by the Hall–Petch effect as a result of the refinement of the structure. However, the raising of the elongation cannot be explained by the Hall–Petch mechanism. The main reason for the improved properties seems more likely to be the result of the non-straightening of bifilm cracks.

From the thermal analysis measurements, in Li-free composite, the favourable formation of Mg<sub>2</sub>Si on bifilms in suspension in the liquid will promote most of the freezing, and the evolution of latent heat, at a relatively high temperature, delaying the general freezing of the alloy (see Fig. 2). As a result of delayed solidification at a higher temperature all the microstructural features will naturally be coarsened.

When modified with an optimum amount of Li, discovered in this study to be close to 0.15 wt.%, the bifilms appear to become deactivated as substrates for the precipitation of both Mg<sub>2</sub>Si particles and eutectic phases. Thus the eutectic no longer nucleates repeatedly on a plentiful supply of substrates on bifilms, but grows at a temperature 10 °C lower, since it has to form on a less favourable nucleus. Furthermore, the less favourable nucleus appears not to be present in large numbers. Thus the growth of the eutectic, having nucleated once, no longer repeatedly nucleates but has to occur as a continuous eutectic solidification controlled by diffusion. This therefore exhibits a finer structure, and would be expected to take on the coral morphology exhibited by modified Al–Si eutectic in Al–Si alloys [26], explaining the rod and dot morphology observed here. The bifilms are now redundant in this new structure. Because they are no longer straightened, they remain in their original compact form, so that strength and elongation are expected to be unimpaired.

Finally, the serrated yielding behaviour observed during tensile extension is a curious feature. Portevin–Le Chateliers' observations of this effect in Al–Mg alloys have been attributed to solute atoms or vacancy interaction with lattice dislocations [31,32]. The effect may be directly related to the interaction of Li atoms with dislocations since Li and Mg atomic radii are approximately similar (0.155 and 0.160 nm, respectively). Alternatively, it seems just possible that the irregularities in yielding might result from the local microscopic failures triggered by the irregular structures of oxides. The masses of double oxide films in the alloy, crumpled to different degrees

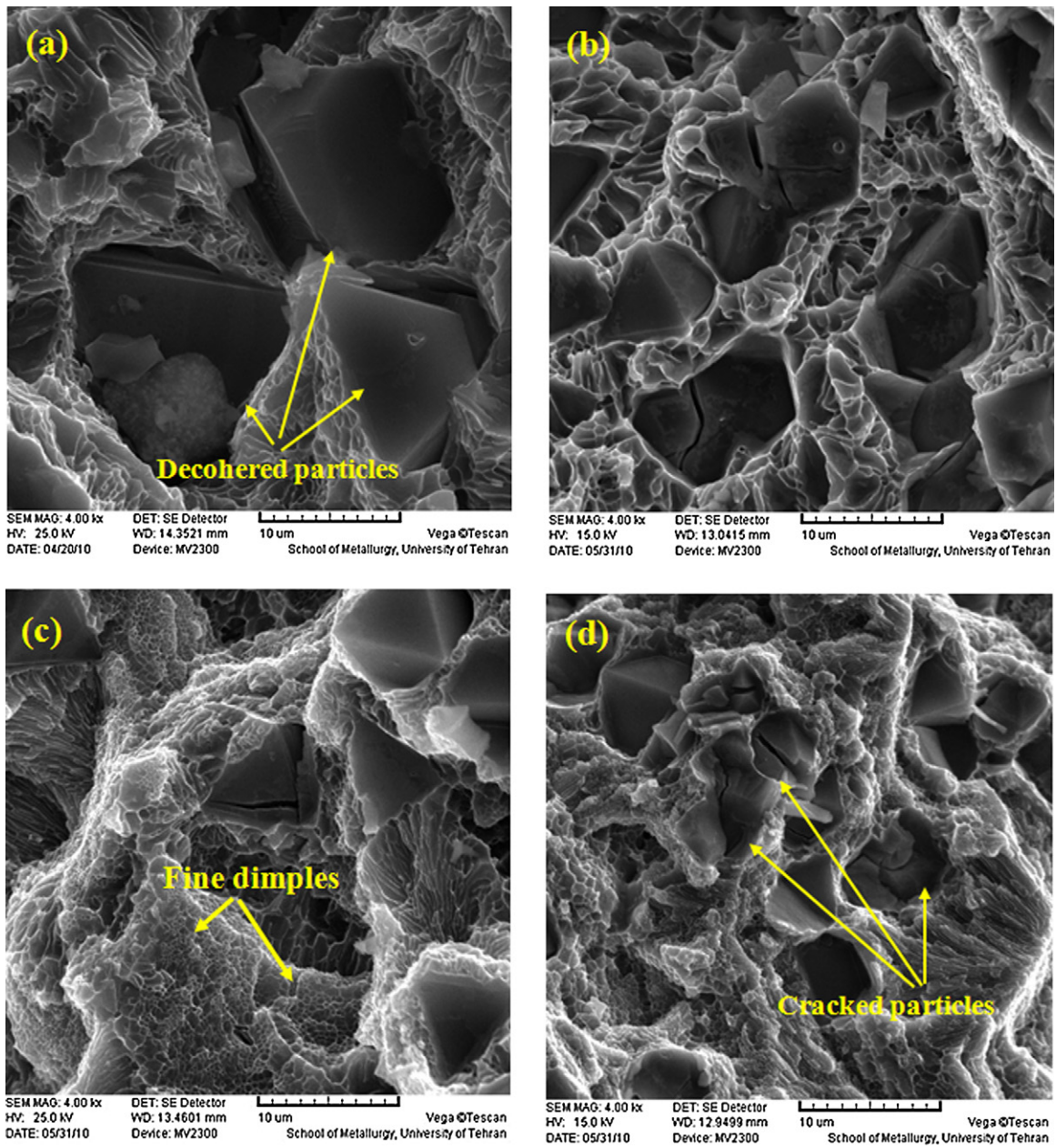


Fig. 10. Fracture surfaces of modified Al–15 wt.%Mg<sub>2</sub>Si composites with different Li contents in high magnification: (a) 0 wt.%, (b) 0.05 wt.%, (c) 0.15 wt.% and (d) 0.25 wt.%.

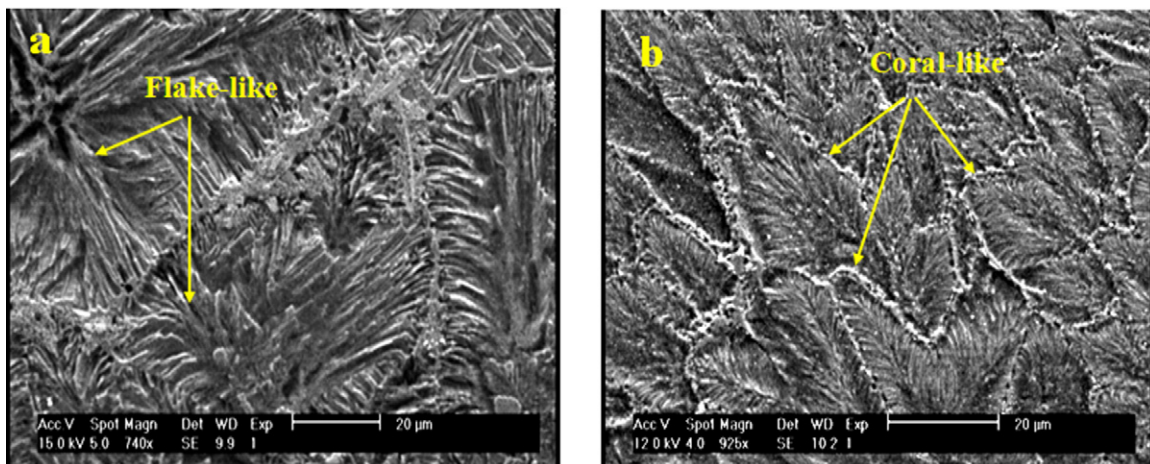


Fig. 11. SEM images of the morphology of the eutectic Mg<sub>2</sub>Si in the composite before and after Li addition: (a) unmodified and (b) modified by 0.15%Li.

by the turbulence of pouring, might be expected to have some such influence on the macroscopic plastic failure of the material. Clearly, their presence as an integral component of the MMC cannot be ignored. A definitive conclusion about their action might have to await the development of bifilm-free Al alloys. Such developments would be welcome.

## 5. Conclusions

The effect of different Li contents on the microstructural and mechanical properties of in situ Al–15% Mg<sub>2</sub>Si composite was investigated and the following conclusions can be deduced: The addition of 0.15 wt.%Li

1. Changes size of primary Mg<sub>2</sub>Si from 32 μm to 4 μm and its morphology from irregular or dendritic to polyhedral.
2. Creates a good distribution of primary Mg<sub>2</sub>Si particles in the matrix.
3. Alters the morphology of the eutectic Mg<sub>2</sub>Si phase from plate-like to coral-like.
4. Increases both UTS and elongation values.
5. Converts the fracture behaviour from brittle, with cleavage facets, to ductile, with fine ductile dimples.
6. All of the morphological and property improvements from the Li addition appear explicable assuming the presence of a high density of oxide bifilms as an unintentional but integral component of the MMC.

## Acknowledgment

The authors would like to thank Universities Tehran and Semnan for financial support during the course of this investigation.

## References

- [1] J. Zhang, Z. Fan, Y. Wang, B. Zhou, Mater. Lett. 18 (1999) 783–784.
- [2] Q.D. Qin, Y.G. Zhao, W. Zhou, P.J. Cong, Mater. Sci. Eng. A 447 (2007) 186–191.

- [3] C.L. Xu, H.Y. Wang, Y.F. Yang, Q.C. Jiang, Mater. Sci. Eng. A 452–453 (2007) 341–346.
- [4] Y.G. Zhao, Q.D. Qin, Y.Q. Zhao, Y.H. Liang, Q.C. Jiang, Mater. Lett. 58 (2004) 2192–2194.
- [5] Q.D. Qin, Y.G. Zhao, Y.H. Liang, W. Zhou, J. Alloys Compd. 399 (2005) 106–109.
- [6] Q.D. Qin, Y.G. Zhao, P.J. Cong, Y.H. Liang, W. Zhou, J. Alloys Compd. 420 (2006) 121–125.
- [7] J. Zhang, Z. Fan, Y.Q. Wang, B.L. Zhou, Mater. Sci. Eng. A 281 (2000) 104–112.
- [8] Y.G. Zhou, Q.D. Qin, W. Zhou, Y.H. Liang, J. Alloys Compd. 389 (2005) L11.
- [9] R. Hadian, M. Emamy, N. Varahram, N. Nemati, Mater. Sci. Eng. A 490 (2008) 250–257.
- [10] Q.D. Qin, Y.G. Zhao, C. Liu, P.J. Cong, W. Zhou, J. Alloys Compd. 454 (2007) 142–146.
- [11] Q.D. Qin, Y.G. Zhao, C. Liu, P.J. Cong, W. Zhou, Y.H. Liang, J. Alloys Compd. 416 (2006) 143–147.
- [12] Q.D. Qin, Y.G. Zhao, J. Alloys Compd. 462 (2008) L228.
- [13] Q.D. Qin, Y.G. Zhao, P.J. Cong, W. Zhou, B. Xu, J. Alloys Compd. A 444 (2007) 99–103.
- [14] Q.D. Qin, Y.G. Zhao, P.J. Cong, Y.H. Liang, W. Zhou, J. Alloys Compd. A 418 (2006) 193–198.
- [15] L. Lu, K.K. Thong, M. Gupta, J. Compos. Sci. Technol. 63 (2003) 627–632.
- [16] C. Li, X. Liu, Y. Wu, J. Alloys Compd. 465 (2008) 145–150.
- [17] J. Zhang, Z. Fan, Y.Q. Wang, B.L. Zhou, J. Mater. Sci. Lett. 19 (2000) 1825–1828.
- [18] N. Zheng, H.Y. Wang, W. Wang, Z.H. Gu, D. Li, Q.C. Jiang, J. Alloys Compd. 459 (2008) L88.
- [19] J. Zhang, Z. Fan, Y.Q. Wang, B.L. Zhou, Scripta Mater. 42 (2000) 1101–1106.
- [20] S.P. Li, S.X. Zhao, M.X. Pan, D.Q. Zhao, X.C. Chen, J. Mater. Sci. 36 (2001) 1569–1575.
- [21] Y.T. Pei, J.Th.M. De Hosson, Acta Mater. 48 (2000) 2617–2624.
- [22] Q.C. Jiang, H.Y. Wang, Y. Wang, B.X. Ma, J.G. Wang, Mater. Sci. Eng. A 392 (2005) 130–135.
- [23] N. Chawla, Y.-L. Shen, Adv. Eng. Mater. 3 (2001) 357–370.
- [24] L. Babout, Y. Brechet, E. Maire, R. Fougères, Acta Mater. 52 (2004) 4517–4525.
- [25] R. Hertzberg, Deformation and Fracture Mechanics, Wiley, 1983, p. 31.
- [26] J. Campbell, M. Tiryakioğlu, Mater. Sci. Technol. 26 (2010) 262–268.
- [27] J. Campbell, Mater. Sci. Technol. 22 (2008) 127–145.
- [28] J. Campbell, Castings, 2nd ed., 2003, pp. 17–31.
- [29] D.N. Miller, L. Lu, A.K. Dahle, Metal. Mater. Trans. B 378 (2006) 873–878.
- [30] J. Campbell, Mater. Sci. Technol. 22 (2006) 127–145.
- [31] J. Segurado, J. Llorca, Acta Mater. 53 (2005) 4931–4942.
- [32] K. Darowicki, J. Orlikowski, Comput. Mater. Sci. 39 (2007) 880–886.